A Multi-Mode Waveguide Tunnel Channel Model for High-Speed Train Wireless Communication Systems

(Invited Paper)

Yu Liu[1], Cheng-Xiang Wang[2], Ammar Ghazal[2], Shangbin Wu[2], Wensheng Zhang[1]
[1]School of Information Science and Engineering, Shandong University, Jinan, Shandong, China
[2]Institute of Sensors, Signals and Systems, Heriot-Watt University, Edinburgh, EH14 4AS, UK
Email: xinwenliuyu@gmail.com, {cheng-xiang.wang, ag289, sw271}@hw.ac.uk, zhangwsh@sdu.edu.cn

***Abstract*—The recent development of high-speed trains (HSTs) introduce new challenges to wireless communication systems for HSTs. For demonstrating the feasibility of these systems, accurate channel models which can mimic key characteristics of HST wireless channels are essential. In this paper, we focus on HST channel models for the tunnel scenario, which is different from other HST channel environments, such as rural area and viaducts. Considering unique characteristics of tunnel channel environments, we extend the existing multi-mode waveguide tunnel channel model to be time dependent, obtain the channel impulse responses, and then further investigate certain key tunnel channel characteristics such as temporal autocorrelation function (ACF) and power spectrum density (PSD). The impact of time on ACFs and PSDs, and the impact of frequency on the received power are revealed via numerical results.**

***Index Terms*—High-speed train, tunnel scenario, multi-mode, waveguide, channel characteristics.**

I. Introduction

In HSTs wireless communication systems, the transmitter (Tx) and receiver (Rx) encounter different channel conditions due to the difference of surrounding geographical environments. There are five typical propagation scenarios: rural macro-cell (RMa), hilly terrain, cutting, viaduct and tunnel [1]. Because of the long limited space, bounding of tunnel, and poor smoothness of the interior wall, propagation characteristics of signals in tunnels are different from other scenarios. Additionally, considering the low cost and low complexity, wireless networks are more efficient than wire-based solutions, and reliable high speed train wireless communication networks in tunnels are essential [2]. However, the radio waves suffer from effects caused by reflections, scattering inside tunnel, and high mobility of train.

To overcome the above problems, and to design an optimal wireless communication network for passengers when the train is in a tunnel, accurate and efficient channel models considering both large-scale and small-scale fading characteristics are crucial. A number of measurement campaigns for tunnels [3], [4] were conducted mainly focusing on large-scale fading parameters. However, small-scale fading parameters were ignored. The characteristics of mobile radio channels inside a tunnel environment have been widely investigated using the geometrical optical (GO) model [5], waveguide model [6], [7], and full wave model [8]. In the GO model, the electromagnetic (EM) field in a tunnel was obtained by summing the ray reflections from tunnel walls and diffractions near the tunnel wedges. It can predict the path loss at any locations as well as the signal delay. The waveguide model considers the tunnel as an oversized waveguide, which characterizes that only lowest mode signal propagate in far region, and ignores the multi-mode case in near region. The full wave model can be derived by solving the Maxwell's equations in arbitrary boundary conditions [9], it has unrealistic computational burden even for a short tunnel path. In [9], a multi-mode model, which combines the existing GO model and waveguide model using Poisson sum formula is developed. It uses a mode matching technique to convert sum of rays of the GO model to the sum of modes by mode intensities. It can characterize the natural wave propagation completely both in near and far regions of the source [9]. Based on the multi-mode model, an in-depth analysis on the tunnel wireless channel characteristics, such as the path loss and root mean squared (RMS) delay spread, is presented. The multi-mode model is also applicable to the tunnels in roads/subways as well as underground mines [9]. This paper aims at extending the exisiting multi-mode channel model and further investigating the small scale channel statistical properties, like the temporal ACF and PSD, and also the received power.

The remainder of this paper is organized as follows. A time dependent multi-mode waveguide tunnel channel model is presented in Section II. In Section III, the statistical properties of the model are derived. The numerical results and the analysis are given in Section IV. Conclusions are drawn in Section V.

II. The multi-mode waveguide tunnel channel model

Tunnel scenario is a special one in all the environments that HST encountered. On a HST railway track, there are usually several tunnels ranging from several hundred meters to several kilometers in length [3], also with shape changing from semicircular sections to rectangular sections. To enable users

inside the train to communicate with the BSs outside smoothly, these tunnels are regarded as parts of cellular networks. Moreover, because of the high communication frequency, the wavelength is much smaller than the transversal dimensions of transportation tunnels, tunnel propagation can be assumed as an oversize waveguide [10].

A. Tunnel channel structure

In this paper, we consider a rectangular tunnel, with cross-sectional dimensions $0 < x < 2a$, $0 < y < 2b$. The coordinate origin is placed in the lower left corner of a cross section at location $z = 0$, which is defined as the initial excitation plane. The moving direction of the train is set to be along the z-axis with a speed of v, and the moving time of train is set to be t. Thus, the instant coordinate at time t in the center can be denoted by $z = v \cdot t$.

For the HST tunnel communication systems, in order to meet the continuous and high quality wireless communication of users on the train, leaky feeders and distributed antennas [4] are the two main ways to achieve tunnel wireless coverage. As leaky feeders are not required special plannings, they have been widely used, but will become more expensive at high operating frequencies [4], and considerable complex in the later maintenance. As a result, solutions based on the use of antennas are becoming more attractive, such as the distributed antenna system (DAS). The distributed antenna elements are connected to a BS via wires or fibers. Compared with leaky feeders, the DAS can provide considerable gain in coverage and capacity, and provide spatial diversity against the fading by using the antenna elements at different locations. It also has advantages in future applications such as higher distance between repeaters, and easy maintenance after being opened [11]. In this paper, a $P \times Q$ MIMO tunnel communication system using the DAS solution is adopted where P is the number transmit antenna elements and Q is the number of mobile receive antenna elements. The system model is described in Fig. 1.

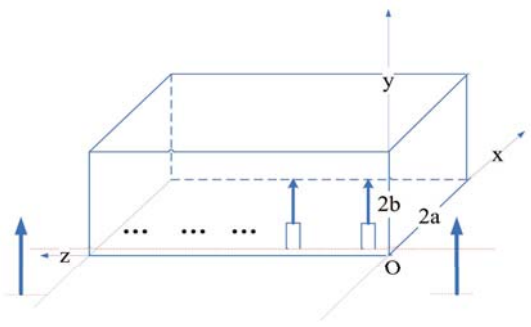

Fig. 1. A rectangular waveguide system model.

B. Modal expansion of rectangular waveguide

In this subsection, we consider the tunnel as a rectangular waveguide and adopt the modal theory to describe the propagation inside the tunnel. In the case of waveguides with perfectly conducting boundaries, the tunnel interior can be regarded as free space, and the walls have complex permittivities. According to the EM theory, two kinds of propagation modes can propagate in a waveguide: the transverse electric (TE) modes and the transverse magnetic (TM) modes, which respectively have a zero component of the electric (E) or magnetic (H) field along z-axis. For the TE modes and TM modes, the x and y components of the E and H modal functions are similar, whereas the z component is different. Each TE or TM mode has a cut-off frequency. In this paper, we take the TM modes as examples to develop our research. At a given operating frequency f_c, only those modes with higher frequency than the cut-off frequency can propagate in a tunnel. Otherwise, all the field components will decay exponentially away from the source of excitation [12]. Due to the size of tunnel is limited, and the cut-off frequency of the fundamental modes is low [3], we can find a wide range of E_{mn} hybrid modes propagating inside the tunnel. If the Tx has a high operating frequency, combining with the given tunnel size, we can calculate that there are a large number of allowable modes. However, in a practical tunnel environment, only certain significant modes can propagate normally since the ceiling and walls are dielectric materials and allow high penetrations [13].

C. The multi-mode waveguide tunnel channel model

The propagation of EM wave in tunnel can be viewed as the superposition of multiple modes with different field distributions and different attenuation coefficients. By solving the Maxwells equations, the expression of the field distributions with each mode can be derived in the form of eigen functions [9], [14], i.e.,

$$e^{\text{eign}}_{m,n}(x_q, y_q) \simeq \sin(\frac{m\pi}{2a}x_q + \varphi_x) \cdot \cos(\frac{n\pi}{2b}y_q + \varphi_y) \quad (1)$$

where (x_q, y_q) denotes the position of receiver along x-axis and y-axis, $\varphi_x = 0$ if m is even and $\varphi_x = \frac{\pi}{2}$ if m is odd. $\varphi_y = 0$ if n is odd and $\varphi_y = \frac{\pi}{2}$ if n is even. Based on [9], the field component $E(x_q, y_q, t)$ of position (x_q, y_q, z) at time t in the tunnel radiated by the pth $(p = 1, 2, \cdots, P)$ transmit element can be calculated as

$$E(x_q, y_q, t) = \sum_{p=1}^{P} \sum_{m} \sum_{n} K_{mn}(x_p, y_p) \cdot e^{\text{eign}}_{m,n}(x_q, y_q) \cdot e^{-(\alpha_{mn} + j\beta_{mn})v \cdot t} \cdot e^{j\omega t} \quad (2)$$

where

$$K_{mn}(x_p, y_p) = \frac{E_0 \cdot \pi}{a \cdot b \cdot \sqrt{1 - (\frac{m\pi}{2ak})^2 - (\frac{n\pi}{2bk})^2}} \cdot \sin(\frac{m\pi}{2a}x_p + \varphi_x) \cos(\frac{n\pi}{2b}y_p + \varphi_y). \quad (3)$$

Here, α_{mn} is the attenuation coefficients, β_{mn} is the phase-shift coefficients, and k is the wave number in tunnel. Thus, the propagation channel from transmitter to receiver can be characterized by the transfer matrix $H_{P\times Q}$ [15]. Each entry $h_{pq}(t)$ of this matrix represents the channel coefficient between the pth transmitter and qth receiver. Because the train moved with a specific speed v along the z-axis, we can denote the arbitrary location z as a function of time t inside tunnel, that is $z = v \cdot t$. The channel impulse response of the tunnel channel model can be expressed as

$$h_{pq}(t) = \sum_{m}\sum_{n} K_{mn}(x_p, y_p) \cdot e^{\text{eign}}_{m,n}(x_q, y_q) \cdot e^{-(\alpha_{mn}+j\beta_{mn})\cdot vt} \cdot e^{j\omega t}. \quad (4)$$

The mode intensity $K_{mn}(x_p, y_p)$ on the excitation plane can be obtained by (3). Once it is determined, the mode propagation can be governed by the tunnel [9].

III. Channel statistical properties

In this section, we will derive the statistical properties of the proposed multi-mode waveguide tunnel model based on the theoretical framework described in Section II.

A. The normalized space-time correlation function (ST CF)

The time correlation properties of two arbitrary channel impulse responses are determined by $h^*_{pq}(t)$ and $h_{pq}(t+\Delta t)$. The normalized time-variant ST CF can be derived as

$$\begin{aligned} R_h(t, \Delta x_T, \Delta x_R, \Delta t) &= \mathrm{E}\left\{h^*_{pq}(t) \cdot h_{p'q'}(t+\Delta t)\right\} \\ &= \mathrm{E}\{\sum_{m}\sum_{n} K_{mn}(x_p, y_p) \cdot e^{\text{eign}}_{m,n}(x_q, y_q) \\ &\quad \cdot e^{-(\alpha_{mn}-j\beta_{mn})\cdot vt} \cdot e^{-j\omega t} \\ &\quad \cdot \sum_{m'}\sum_{n'} K_{m'n'}(x_{p'}, y_{p'}) \cdot e^{\text{eign}}_{m',n'}(x_{q'}, y_{q'}) \\ &\quad \cdot e^{-(\alpha_{m'n'}+j\beta_{m'n'})\cdot v(t+\Delta t)} \cdot e^{j\omega(t+\Delta t)}\}. \end{aligned} \quad (5)$$

The position of the pth $(p = 1, 2, \cdots, P)$ element of the Tx denoted by (x_p, y_p, z), the antenna spacings in Tx is Δx_T, and the position of the qth $(q = 1, 2, \cdots, Q)$ element of Rx is denoted by (x_q, y_q, z), the antenna spacings in Rx is Δx_R. Both antenna spacings are just related to the position of antennas in Tx, Rx, that is $x_{p'} = x_p + \Delta x_T$, $x_{q'} = x_q + \Delta x_R$. Here, by imposing $\Delta x_T = 0$ and $\Delta x_R = 0$ in (5), we can get the normalized temporal ACF, i.e.,

$$\begin{aligned} r(t, \Delta t) &= R_h(t, 0, 0, \Delta t) \\ &= \mathrm{E}\{\sum_{m,n} K_{mn}(x_p, y_p) \cdot e^{\text{eign}}_{m,n}(x_q, y_q) \\ &\quad \cdot e^{-(\alpha_{mn}-j\beta_{mn})\cdot vt} \cdot e^{-j\omega t} \\ &\quad \cdot \sum_{m',n'} K_{m'n'}(x_p, y_p) \cdot e^{\text{eign}}_{m',n'}(x_q, y_q) \\ &\quad \cdot e^{-(\alpha_{m'n'}+j\beta_{m'n'})\cdot v(t+\Delta t)} \cdot e^{j\omega(t+\Delta t)}\}. \end{aligned} \quad (6)$$

In [12], it was pointed out that the modes in a rectangle tunnel approximately satisfy the orthogonality, i.e.,

$$\int\int e^{\text{eign}}_{m,n}(x, y) e^{\text{eign}}_{m',n'}(x, y) = \begin{cases} \zeta^2 & \text{if } m = m', n = n' \\ 0 & \text{otherwise} \end{cases} \quad (7)$$

where ζ is the norm of modes. By imposing (7) in (6), we can obtain the simplified temporal ACF as,

$$r(t, \Delta t) = \sum_{m,n} K^2_{mn}(x_p, y_p) \cdot \zeta^2 \cdot e^{-2\alpha_{mn}\cdot vt - \alpha_{mn}\cdot v\Delta t} \cdot e^{-j\beta_{mn}\cdot v\Delta t + j\omega\Delta t}. \quad (8)$$

B. Doppler PSD

The Doppler PSD $W(t, f)$ with respect to the Doppler frequency f is the Fourier transform of the temporal ACF which can be presented as

$$\begin{aligned} W(t, f) &= \int_{-\infty}^{\infty} r(t, \Delta t) \cdot e^{-j2\pi f\cdot\Delta t} d\Delta t \\ &= \sum_{m,n} K^2_{mn}(x_p, y_p) \cdot \zeta^2 \cdot e^{-2\alpha_{mn}\cdot vt} \\ &\quad \cdot \frac{e^{(-\alpha_{mn}\cdot v - j\beta_{mn}\cdot v + j\omega - j2\pi f)\cdot\tau_{\max}} - 1}{-\alpha_{mn}v - j\beta_{mn}v + j\omega - j2\pi f}. \end{aligned} \quad (9)$$

It should also be noticed that the Doppler PSD is time dependent.

C. Received power

By imposing the channel impulse response in (4), the received power can be derived as

$$P(t) = |h_{pq}(t)|^2 = \sum_{m}\sum_{n} K^2_{mn}(x_p, y_p) \cdot \zeta^2 \cdot \left| e^{-2\alpha_{mn}\cdot vt} \cdot e^{-j(\beta_{mn}\cdot vt - \omega t)} \right|^2. \quad (10)$$

IV. Numerical results and analysis

In this section, the statistical properties of the proposed multi-mode tunnel channel model are evaluated and analyzed, such as temporal ACF and PSD. The tunnel cross section shape is rectangular with a width of $2a$ and a height of $2b$; the tunnel wall, ceiling and floor are treated as uniform and lossless, made of same material with electrical parameters $\varepsilon = 5$, $\sigma = 0.01$ S/m; the tunnel interior is filled with normal air $\varepsilon = 1$, $\sigma = 0$ S/m. Refer to [4], the transmitters of the DAS are installed at 4 m above the floor, 25 cm from the tunnel walls, with the operating frequencies at 2.4 GHz. Here, we take a SISO system as example, just consider the communication link between the pth transmitter and the qth receiver, set the origin of coordinates at $(0, 0, 0)$, the location of the transmitter at coordinate $(x_p, y_p, z) = (0.25, 4, 0)$, and observation point at the coordinate $(x_q, y_q, z) = (2.2, 4, z)$. The train moved with a specific speed in the specific direction along the z-axis. We assume that the field at the transmitter is E_0.

The absolute value of the resulting generalized temporal ACF $r(t, \Delta t)$ is illustrated in Fig. 2. From the figure, we can

observe the approximately same shape of temporal ACF at different time instant t, which relates to the time difference Δt, rather than the time instant t. From all the above, we can conclude that the wide-sense stationary assumption would be sufficient to meet. Fig. 3 shows the absolute values of temporal ACFs in choosing different tunnel size. Basically, the existing modes in a waveguide depend on tunnel size and operating frequency [9]. Here, a group of important comparisons of the ACF between tunnel size I (4.8 m $\times$ 6.2 m) and tunnel size II (9.8 m $\times$ 6.8 m) with same conditions have been made. We select different sizes of tunnel, then determine the significant mode values that can propagate in tunnel. It can be seen from the corresponding simulation results that the ACFs have a highly difference between tunnel size I and tunnel size II [16], [17]. In Fig. 4, it shows the absolute values of temporal ACFs in choosing different mode values, including the single-mode and multi-modes. From this figure, we can see that as the number of mode increases, the correlation decreases. As a result, the capacity will increase with the number of modes and this agrees with [15].

From Fig. 6, we can observe that the received power curve among the significant modes as a function of t at frequencies of 2.4 GHz [4] and 930 MHz [3], [18]. It can be seen that the signal attenuates as time goes on. Due to multiple modes operating, signal experiences serious fluctuations in the specific tunnel space [9], and different operating frequencies will also have a significant influence on the signal power distribution. Because the operating frequency impacts on the propagation constants, inducing that signals with a higher frequency will attenuate slower [9]. Fig. 7 shows the received power along the multi modes and single mode cases. From this figure, we can observe that the single mode, i.e., the lowest order mode $m = n = 1$, experiences less attenuation than higher order modes [15]. We can also calculate the received power by summating all the significant single modes [9].

V. Conclusions

In this paper, we have proposed a time related multi-mode high-speed train tunnel channel model based on the existing multi-mode waveguide model [9] for wireless networks in tunnels. By applying modal analysis of EM waves and considering the waveguide effect into tunnel channel modeling, we have proposed a deterministic tunnel channel model, which enables us to study the channel characteristics. From this model, we have derived the temporal ACF, the PSD, and the received power. Numerical analyses have shown how the ACF changes with different time instants t and different tunnel sizes. This has demonstrated that the ACF is related to the tunnel size, rather than the time-variant effect. Moreover, we have also analyzed the trends of power change along the Doppler frequencies at different time instants t, and the received power at different operating frequencies and different modes. It has been illustrated that different operating frequencies will have significant impact on the received power.

Acknowledgements

The authors would like to acknowledge the support of the 863 project in 5G, Ministry of Science and Technology (Grant No. SS2014AA01A707), the QUICK project, International Research Staff Exchange Scheme (FP7-PEOPLE-2013-IRSES), European Commission, Natural Science Foundation of China (Grant No. 61371110), and the General and Special Program of China Postdoctoral Science Foundation (Grant No. 2012M521334 and 2013T60669).

References

[1] A. Ghazal, C.-X. Wang, B. Ai, D. Yuan, and H. Haas, "A non-stationary wideband MIMO channel model for high-mobility intelligent transportation systems," *IEEE Trans. Intell. Transp. Syst.*, vol. 16, no. 1, Feb. 2015.

[2] M. Lienard, S. Betrencourt, and P. Degauque, "Propagation in road tunnels: a statistical analysis of the field distribution and impact of the traffic," *Ann. Telecom.*, vol. 55, no. 11-12, pp. 623–631, Dec. 2000.

[3] C. Briso-Rodriguez, J. M. Cruz, and J. I. Alonso, "Measurements and modeling of distributed antenna systems in railway tunnels," *IEEE Trans. Veh. Technol.*, vol. 56, no. 5, pp. 2870–2879, Sept. 2007.

[4] K. Guan, Z. D. Zhong, J. I. Alonso, and C. Briso-Rodriguez, "Measurement of distributed antenna system at 2.4GHz in a realistic subway tunnel environment," *IEEE Trans. Veh. Technol.*, vol. 61, no. 2, pp. 834–837, Feb. 2012.

[5] S. F. Mahmoud and J. R. Wait, "Geometrical optical approach for electromagnetic wave Propagation in rectangular mine tunnels," *Radio Science*, vol. 9, no. 12, pp. 1147–1158, Dec. 1974.

[6] A. G. Emslie, R. L. Lagace, and P. F. Strong, "Theory of the propagation of UHF radio waves in coal mine tunnels," *IEEE Trans. Antenna Propag.*, vol. AP-23, no. 2, pp. 192–205, Mar. 1975.

[7] Y. P. Zhang, "A Novel model for propagation loss prediction in tunnels," *IEEE Trans. Veh. Technol.*, vol. 52, no. 5, pp. 1308–1314, Sept. 2003.

[8] A. Taflove and S. C. Hagness, Computational Electrodynamics: *The Finite-Difference Time-Domain Method, 3rd edition.* Norwood. MA: Artech House, 2005.

[9] Z. Sun and I. F. Akyildiz, "Channel modeling and analysis for wireless networks in underground mines and road tunnels," *IEEE Trans. Commun.*, vol. 58, no. 6, pp. 1758–1768, Jun. 2010.

[10] Y. P. Zhang and Y. Hwang, "Theory of the radio-wave propagation in railway tunnels," *IEEE Trans. Veh. Technol.*, vol. 47, no. 3, pp. 1027–1036, Aug. 1998.

[11] K. Guan, Z. D. Zhong, and B. Ai, "Statistic modeling for propagation in tunnels based on distributed antenna systems," in *Proc. IEEE APSURSI*, Florida, USA, Jul. 2013, pp. 1920–1921.

[12] S. Loyka, "Multiantenna capacities of waveguide and cavity channels," *IEEE Trans. Veh. Technol.*, vol. 54, no. 3, pp. 863–872, May 2005.

[13] D. Porrat, "Radio propagation in hallways and streets for UHF communications," Ph.D. thesis, Stanford University, Dec. 2002.

[14] K. D. Laakmann and W. H. Steier, "Waveguides: characteristic modes of hollow rectangular dielectric waveguides," *Appl. Opt.*, vol. 15, pp. 1334–1340, May 1976.

[15] J. M. G. Pardo, M. Lienard, P. Degauque, D. G. Dudley, and L. Juan-Llacer, "Interpretation of MIMO channel characteristics in rectangular tunnels from modal theory," *IEEE Trans. Veh. Technol.*, vol. 57, no. 3, pp. 1974–1979, May 2008.

[16] A. Chelli and M. Patzold, "A non-stationary MIMO vehicle-to-vehicle channel model based on the geometrical T-Junction model," in *Proc. IEEE WCSP09*, Nanjing, China, Nov. 2009, pp. 1–5.

[17] N. Avazov and M. Patzold, "A wideband car-to-car channel model based on a geometrical semicircular tunnel scattering model," in *Proc. PIMRC13*, London, United Kingdom, Sept. 2013, pp. 253-258.

[18] B. Chen, Z. Zhong, and B. Ai, "Stationarity intervals of time-variant channel in high speed railway scenario," *J. China Commun.*, vol. 9, no. 8, pp. 64–70, Aug. 2012

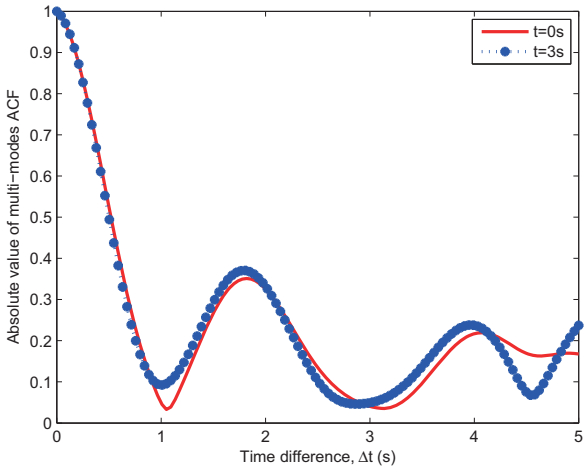

Fig. 2. Comparison between the time-variant ACFs of multi-modes model with different time instants ($2a = 4.8$ m, $2b = 5.3$ m, $f_c = 2.4$ GHz, $v_R = 360$ km/h, $m = 1:4$, $n = 1:4$).

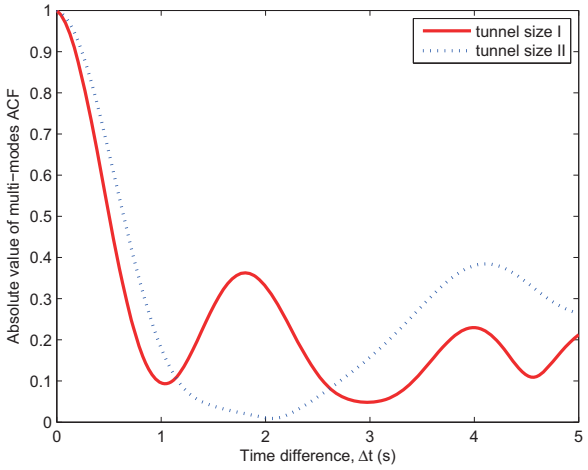

Fig. 3. Comparison between the time-variant ACFs of multi-modes model with different tunnel sizes ($f_c = 2.4$ GHz, $v_R = 360$ km/h, tunnel size I: $2a_1 = 4.8$ m, $2b_1 = 5.3$ m, $m_1 = 1:4$, and $n_1 = 1:4$, tunnel size II: $2a_2 = 9.8$ m, $2b_2 = 6.8$ m, $m_2 = 1:6$, and $n_2 = 1:6$).

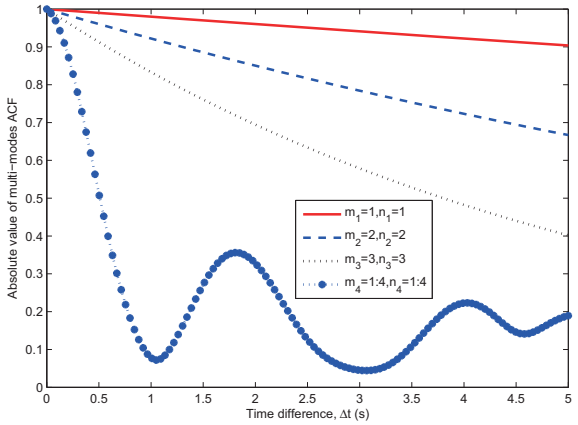

Fig. 4. Comparison between the time-variant ACFs of multi-modes model with different tunnel sizes ($2a = 4.8$ m, $2b = 5.3$ m, $f_c = 2.4$ GHz, $v_R = 360$ km/h, single mode: $m_1 = 1$, $n_1 = 1$, $m_2 = 2$, $n_2 = 2$, $m_3 = 3$, $n_3 = 3$, multi modes: $m_4 = 1:4$, $n_4 = 1:4$).

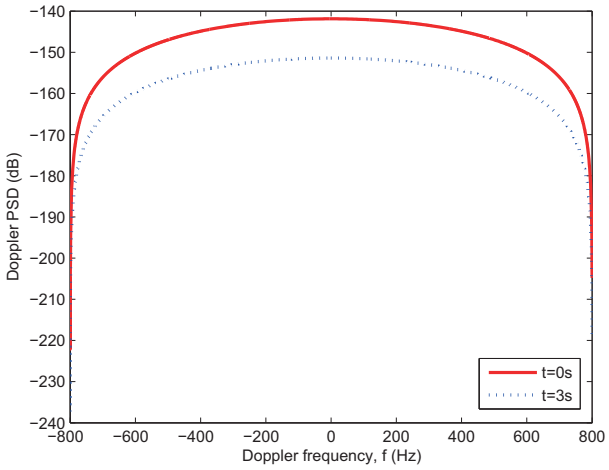

Fig. 5. Comparison between the PSDs of multi-modes model with different time instants ($2a = 4.8$ m, $2b = 5.3$ m, $f_c = 2.4$ GHz, $v_R = 360$ km/h, $m = 1:4$, $n = 1:4$).

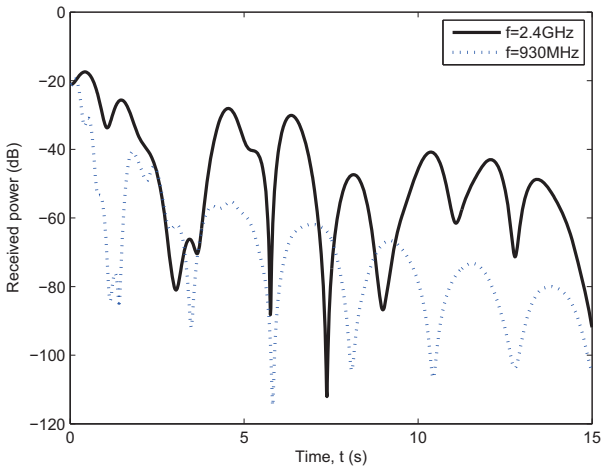

Fig. 6. Comparison between the received power of multi-mode model with different operating frequencies ($2a = 4.8$ m, $2b = 5.3$ m, $v_R = 360$ km/h, $m = 1:4$, $n = 1:4$, $f_{c1} = 2.4$ GHz, $f_{c2} = 930$ MHz).

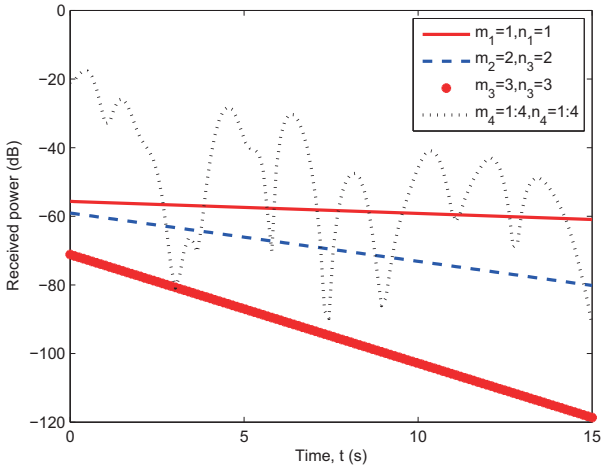

Fig. 7. The received power of multi-modes model for different mode values ($2a = 4.8$ m, $2b = 5.3$ m, $v_R = 360$ km/h, $f_c = 2.4$ GHz, single mode: $m_1 = 1$, $n_1 = 1$, $m_2 = 2$, $n_2 = 2$, $m_3 = 3$, $n_3 = 3$, multi modes: $m_4 = 1:4$, $n_4 = 1:4$).